Topological Superconducting State of Lead Nanowires in an External Magnetic Field

J. G. Rodrigo,[1] V. Crespo,[1] H. Suderow,[1] S. Vieira,[1] and F. Guinea[2]

[1]*Laboratorio de Bajas Temperaturas, Departamento de Física de la Materia Condensada, Instituto de Ciencia de Materiales Nicolás Cabrera, Facultad de Ciencias, Universidad Autónoma de Madrid, E-28049 Madrid, Spain*

[2]*Instituto de Ciencia de Materiales de Madrid, CSIC Sor Juana Inés de la Cruz 3, E-28049 Madrid, Spain*

(Received 21 March 2012; published 4 December 2012)

Superconductors with an odd number of bands crossing the Fermi energy have topologically protected Andreev states at interfaces, including Majorana states in one-dimensional geometries. We propose here that repeated indentation of a Pb tip on a Pb substrate can lead to nanowires such that the resulting superconducting system has novel topological properties. We have analyzed a number of conductance curves obtained in different nanowires, and observe, in a few cases, very peculiar dependence of the critical current on magnetic field. In these cases, the form of multiple Andreev reflections observed at finite voltages are compatible with topological superconductivity. The nanowires give a low number of 1D channels, large spin orbit coupling, and a sizable Zeeman energy, provided that the applied magnetic field is higher than the Pb bulk critical field.

DOI: 10.1103/PhysRevLett.109.237003 PACS numbers: 74.78.Na, 73.63.Nm, 74.25.−q, 74.81.Fa

A number of materials have band structures which support edge and surface states with unusual charge and spin transport properties [1–3]. These materials include generalized integer quantum Hall systems, topological insulators, and topological superconductors. The excitations at the edges of one-dimensional topological superconductors can be described as Majorana particles [4–6]. The exchange of two such states leads to a nontrivial modification of the state of the system. The simplest realization of a topological superconducting state requires [4–13] (i) a small number of conduction channels, (ii) a band structure modified by spin-orbit coupling, (iii) an interaction which leads to the formation of Cooper pairs, and (iv) a sufficiently strong Zeeman coupling to an external magnetic field. The ingredients described above are present in lead nanowires a few angstroms wide in the presence of a magnetic field higher than the bulk critical field [14–19]. They can give rise, under the right conditions discussed below, to a zero bias conductance peak. The electrical conductance of metallic contacts of nanoscopic dimensions can be obtained in terms of the contributions of 1D quantum conduction channels. In the particular case of superconducting nanocontacts, the number of 1D channels involved in the conduction, and their individual transmissions, can be determined in detail through the analysis of the features emerging in the spectroscopic curves due to Andreev reflection processes [20–23].

The system studied here is sketched in Fig. 1. A narrow and elongated constriction between two lead electrodes is built by carefully stretching an STM tip away from a substrate. Close to the breaking point, the number of conducting channels is small, of the order of one, and their individual transmissions can be obtained from the analysis of the features due to multiple Andreev reflections (MAR) in the spectroscopic curves. The superconducting properties of the electrodes and the constriction are modified in an applied magnetic field. The system continues to exhibit a Josephson current at zero voltage and MAR peaks at fields larger than the bulk critical field, H_c. At these fields the electrodes are in the normal state, and superconductivity is restricted to the constriction, where orbital currents cannot quench superconductivity. The resulting device can be seen as a nanoscopic Josephson junction, with a weak link where the voltage drop occurs. The magnetic field also induces a Zeeman splitting on the electrons in the constriction.

As the two electrodes are unequal, the magnetic field is more effective in changing the superconducting features in one of them, which eventually becomes normal. When this happens, the superconducting gap is lowered, and a significant Zeeman shift of the bands can be expected. Spin-orbit coupling in lead is large, and the estimated g factors for bulk lead are in the range $g \approx 4$–6 [24,25], which can

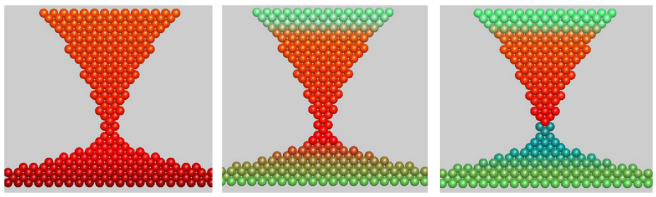

FIG. 1 (color online). Sketch of the nanostructure and nanoelectrodes (tip and sample) involved in the experiments. The superconducting region is colored red. Left: At low applied magnetic fields, $H \ll H_c$, where H_c is the bulk critical field of lead, the whole structure is in the superconducting state. Center: For $H \geq H_c$ the bulk electrodes are in normal state (green), superconductivity is restricted to the region near the junction, and the device shows a finite Josephson current. Right: Increasing the magnetic field, superconductivity survives at the nanotip, while the nanostructure on the sample becomes a topological superconductor (blue).

be enhanced by interaction effects in nanoscopic samples [26]. For fields in the range $\mu_0 H \approx 0.1$–0.2 T, the Zeeman splitting, B, can be of order of 0.04–0.06 meV, while the superconducting gap, $\Delta = 1.35$ meV at zero field and zero temperature, is expected to go smoothly to zero as the magnetic field increases. Hence, a regime where the Zeeman coupling is larger than the superconducting gap can exist in some of the nanowires studied here. Topological superconductivity requires that the Fermi energy lies within the Zeeman gap induced by the magnetic field. The position of the Fermi energy at the constriction depends on details of the electrostatic potential which, in turn, is determined by the geometry of the contact. We expect that the Fermi energy is within the Zeeman gap in a fraction of the samples studied, due to random fluctuations in the electrostatic potential.

When the right combination of parameters is achieved, the Zeeman coupling will open a gap near the Fermi level, so that the number of pairs of bands crossing the Fermi energy will be odd on one side of the constriction. These are the conditions required for topological superconductivity to exist. The constriction becomes a boundary between a topological and a nontopological superconductor, S-S_T. A midgap state with particle-hole character will be formed there. Another broad resonance with mixed particle-hole character is expected at the N-S_T interface where the superconducting features disappear away from the constriction. The two resonances will be hybridized and changed into conventional Andreev states when they are closer than the superconducting coherence length. If the coupling between the two states can be neglected, the midgap state at the constriction has all the features of a Majorana particle. The regions S and S_T have random rough edges. They are in the diffusive regime, with an elastic mean free path, ℓ, comparable to their width W. Hence, a Majorana fermion at the constraint will be well defined if the length of the S_T region, L, is such that $L \geq \sqrt{\xi \ell} \approx \sqrt{\xi W}$, where $\xi \approx 80$ nm is the coherence length in clean lead.

In the experiments, indentations, in the range of a few tens of nanometers, of a Pb tip on a Pb sample are induced, in order to fabricate sharp elongated nanotips and nanoprotrusions on the sample surface. The experiments on the resulting nanostructures are performed at 0.3 K, with the STM installed in a ^{3}He cryostat equipped with a superconducting solenoid to apply a magnetic field. The evolution of the electronic and superconducting properties of the nanostructure versus magnetic field can be followed from the analysis of the conductance characteristics of the constriction. During the magnetic field sweeps, the STM feedback loop is kept active, at fixed bias voltage, typically 10 mV, with a constant value for the current across the constriction, in order to ensure that the overall geometry of the nanostructure is not altered along the process. The feedback loop is blocked during the acquisition of the current vs voltage curves. Different nanostructures, with conductance values at the constriction ranging from $2G_0$ to $50G_0$ ($G_0 = 2e^2/h$ is the conductance quantum) were studied. The numeric derivative of the I-V curves acquired during the magnetic field sweeps gives the conductance, where the signatures of the different Andreev reflection processes can be easily identified. The presence of Josephson current, a finite current at zero bias, reflects a sharp peak in the conductance curves at zero bias. The I-V characteristics in the absence of Zeeman coupling shows distinct features at $eV = \Delta + \Delta'$ and at $eV = \Delta - \Delta'$, where Δ and Δ' are the superconducting gaps at the two regions at each side of the junction.

In order to investigate the phenomenon described above, a nanocontact with low conductance ($G \sim 3G_0$) is created at zero magnetic field, and its electronic and superconducting properties are followed as a function of the magnetic field. We focus on the variations with field of the conductance of the junction, the value of the Josephson critical current, and the detail of the Andreev reflection features present in the conductance curves, as shown in Fig. 2.

The I-V curves obtained at zero field are fitted to the MAR model to obtain the number of conducting channels and its transmission values. Following the procedure described in Ref. [27] we get that four channels, with transmission values 1, 0.920, 0.600, and 0.225 account for 99.5% of the current, being the contribution of other channels below 0.005, which is the limit of the resolution in the fitting. This result indicates that the condition requiring a small number of conducting channels to observe

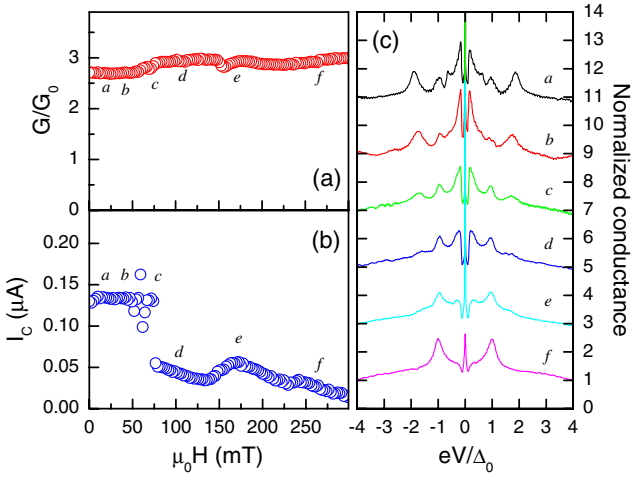

FIG. 2 (color online). Evolution of the conductance, (a), and Josephson current, (b), of a small constriction ($G \approx 3G_0$) as a function of the applied magnetic field. Note the bump of the Josephson current at ≈ 175 mT. In (c) we present several conductance curves obtained along the field sweep. The field values corresponding to the curves are indicated with the labels a-f in panels (a) and (b). (Δ_0 is the value of the superconducting gap of lead at zero field, 1.35 meV. Curves are shifted vertically 2 units for clarity.)

Majorana particles is fulfilled. Occasionally, slight atomic rearrangements at the nanocontact take place. These rearrangements are seen as variations in the conductance and the Josephson current [28,29], which can be directly related to slight changes in the conduction channel arrangements through the contact and have no influence in the behavior discussed.

When the magnetic field is swept up to its bulk critical value (75 mT at 300 mK), the conductance curves keep similar MAR features [curves (a), (b) in Fig. 2(c)]. The crossing of H_c results in a reduction of the MAR related current, and in the voltage position of the characteristic peaks. The Josephson critical current decreases sharply to about half of its value below H_c. The magnetic field is reducing more effectively the superconducting features in one of the nanoelectrodes. This results in a slight upturn in the conductance, which can be related to asymmetric changes in the excess current. As field is increased significantly above H_c the MAR features and the Josephson critical current are progressively reduced until about 135 mT, where we detect an unexpected rise of the critical current, with a maximum at 175 mT and a continuous decrease at higher fields. This is accompanied by the evolution of the Andreev reflection signature in the conductance curves towards a situation where only one of both parts is superconducting, namely a S-N situation. Although no signature of S-S superconductivity is found in the conductance curves, a well-defined Josephson-like signature at zero bias [curves (d)–(f) in Fig. 2(c)] is observed up to $4H_c$.

We checked the robustness of this observation by repeating the field sweeps. The ''anomalous'' bump in the evolution of the Josephson current at high field was observed several times, until in one of the sweeps the abovementioned atomic rearrangements led to the situation presented in Fig. 3. After these rearrangements, at about 40 mT, the nanocontact presented higher conductance but a clearly smaller Josephson critical current. The characteristics of the conducting channels before and after the rearrangements were obtained as above, and we find that in the new configuration up to eight channels contribute with transmission values above 0.1, being less than 0.4 for five of them [28]. As the field is further increased we obtain the evolution of the conductance curves and the Josephson critical current expected within a conventional magnetic pair breaking induced destruction of superconductivity. In other nanostructures, there is a sharp jump in I_C at H_c followed by a progressive reduction of the MAR signature and the value of I_C, until 130 mT where the conductance curves present a S-N-type Andreev reflection behavior, and no Josephson-like feature can be detected at zero bias. In the case presented in Fig. 3, the result is identical to the results obtained for contacts with a large amount of conduction channels and conductances in the range of $50G_0$ and above [28].

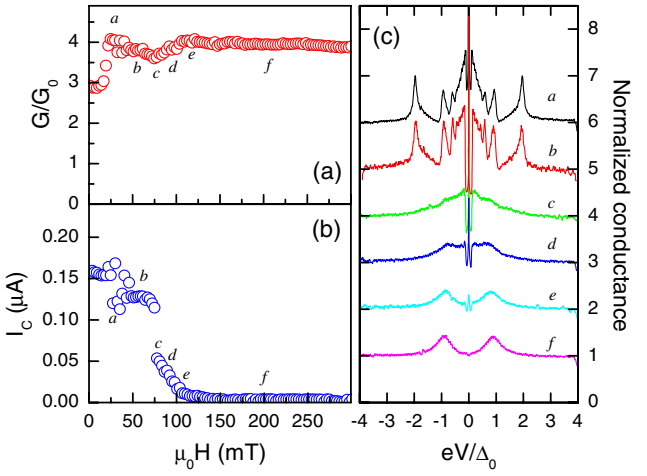

FIG. 3 (color online). Evolution of the conductance, (a), and Josephson current, (b), of a small constriction ($G \approx 4G_0$) as a function of the applied magnetic field. In (c) we present several conductance curves obtained along the field sweep. The field values corresponding to the curves are indicated with the labels a-f in panels (a) and (b). (Δ_0 is the value of the superconducting gap of lead at zero field, 1.35 meV. Curves are shifted vertically 1 unit for clarity.)

We have modeled the above results by generalizing MAR scattering theory to a partially open channel which connects a topological, S_T, and a nontopological superconductor, S [28,30]. In the model we assume that the superconducting and Zeeman gaps can be different at the two electrodes (Δ, Δ', B, B'). Typical examples are shown in Fig. 4. The high voltage structure is washed out as the Zeeman coupling increases, and a single feature at about the value of the highest superconducting gap remains for Zeeman couplings near and above the transition. As the magnetic field is increased, the dependence of the Josephson current on the transmission coefficient evolves from $I_c \propto T$ in the S-S' regime, to $I_c \propto \sqrt{T}$ in the S_T-S'_T regime [31] (for $T \ll 1$) leading to a minimum in I_c in the S-S'_T regime. The suppression of structure in the I-V curves at high voltages, and the minimum in the value of the critical current can be explained by the existence of a junction between a nontopological and topological superconductor.

It is finally worth noting that the devices which show the unconventional combination of a finite Josephson current and single Andreev reflection characteristics at finite voltages (N-S behavior) present few (~ 3) channels as determined from the MAR characteristics at zero field.

The results presented here suggest that boundaries between topological and nontopological superconductors can be found in lead constrictions with a small amount of conduction channels (see also Ref. [32]). Metallic devices are not expected to show topological superconductivity because of the high density of states and number of channels. Both features can be eliminated using nanofabricated

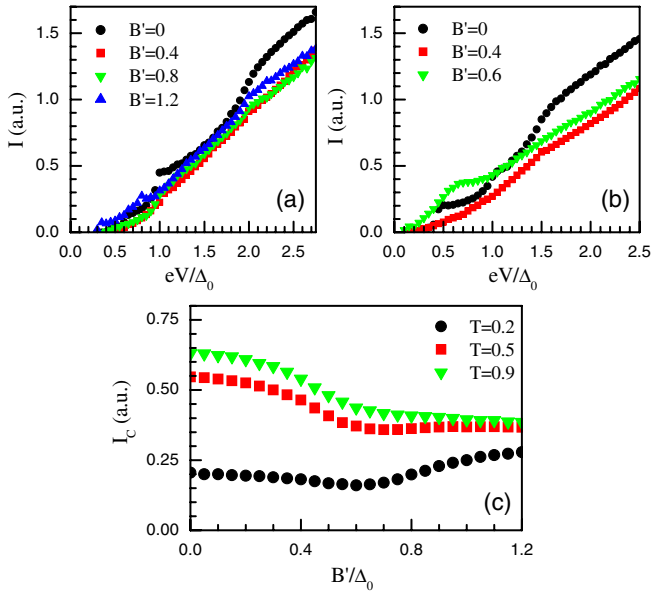

FIG. 4 (color online). Calculated I-V curves of junctions with different values of the Zeeman coupling. (a): $\Delta = \Delta' = 1$. (b): $\Delta = 1$, $\Delta' = 0.5$. (c): Critical current as function of Zeeman coupling, B', for a superconducting junction with $\Delta = 0.8$, $\Delta' = 0.5$ and different transmissions (see the Supplemental Material [28]). The junction type is S-S' for $0 \leq B' \leq 0.4$, S-S_T for $0.4 \leq B' \leq 0.8$, and S_T-S'_T for $0.8 \leq B'$. (Δ, Δ', and B' are expressed in units of Δ_0.)

constrictions. The number of conducting channels can be determined with high precision, by means of Andreev reflection features. When only small channels are open, midgap states giving rise to Majorana fermions can exist at boundaries. The nanoconstrictions studied here show simultaneously superconductivity, few channels, strong spin-orbit coupling, and a large modification of the superconducting features by a magnetic field. Of course, statistics is here a key factor to find the few cases where all needed interactions act at the same time. However, these junctions can be fabricated in large numbers, and it is expected that, some of them showing the features identified here, may have the right values for the existence of Majorana fermions. Knowledge about channel number and transparency, statistics and spin-orbit coupling are the keys which make these systems an alternative to other materials currently under study in the search for Majorana fermions in condensed matter physics [33,34].

The Laboratorio de Bajas Temperaturas is associated to the ICMM of the CSIC. This work was supported by the Spanish MINECO (Consolider Ingenio Molecular Nanoscience CSD2007-00010 program, FIS2011-23488), by the Comunidad de Madrid through program Nanobiomagnet. F. G. acknowledges funding from Grants No. FIS2008-00124 and No. FIS2011-23713 and from the ERC Advanced Grants program, Contract No. 290846. This research was supported in part by the National Science Foundation under Grant No. NSF PHY11-25915. F. G. acknowledges useful conversations with E. Prada, P. San Jose, and B. Trauzettel.

Note added.—Recently, evidence for Majorana states has been reported in InSb wires [35].

[1] F. D. M. Haldane, Phys. Rev. Lett. **61**, 2015 (1988).
[2] M. Z. Hasan and C. L. Kane, Rev. Mod. Phys. **82**, 3045 (2010).
[3] X.-L. Qi and S.-C. Zhang, Phys. Today **63**, No. 1, 33 (2010).
[4] J. D. Sau, R. M. Lutchyn, S. Tewari, and S. Das Sarma, Phys. Rev. Lett. **104**, 040502 (2010).
[5] Y. Oreg, G. Refael, and F. von Oppen, Phys. Rev. Lett. **105**, 177002 (2010).
[6] R. M. Lutchyn, J. D. Sau, and S. Das Sarma, Phys. Rev. Lett. **105**, 077001 (2010).
[7] A. C. Potter and P. A. Lee, Phys. Rev. Lett. **105**, 227003 (2010).
[8] A. C. Potter and P. A. Lee (to be published).
[9] A. C. Potter and P. A. Lee, Phys. Rev. B **83**, 094525 (2011).
[10] R. M. Lutchyn, T. D. Stanescu, and S. Das Sarma, Phys. Rev. Lett. **106**, 127001 (2011).
[11] P. W. Brouwer, M. Duckheim, A. Romito, and F. von Oppen, Phys. Rev. B **84**, 144526 (2011).
[12] K. T. Law and P. A. Lee, Phys. Rev. B **84**, 081304 (2011).
[13] J. Alicea, Y. Oreg, G. Refael, F. von Oppen, and M. P. A. Fisher, Nat. Phys. **7**, 412 (2011).
[14] C. Untiedt, G. Rubio, S. Vieira, and N. Agrait, Phys. Rev. B **56**, 2154 (1997).
[15] M. Poza, E. Bascones, J. G. Rodrigo, N. Agrait, S. Vieira, and F. Guinea, Phys. Rev. B **58**, 11 173 (1998).
[16] H. Suderow, E. Bascones, W. Belzig, F. Guinea, and S. Vieira, Europhys. Lett. **50**, 749 (2000).
[17] H. Suderow, E. Bascones, A. Izquierdo, F. Guinea, and S. Vieira, Phys. Rev. B **65**, 100519 (2002).
[18] J. G. Rodrigo, H. Suderow, and S. Vieira, Phys. Status Solidi B **237**, 386 (2003).
[19] J. G. Rodrigo, H. Suderow, S. Vieira, E. Bascones, and F. Guinea, J. Phys. Condens. Matter **16**, R1151 (2004).
[20] E. N. Bratus', V. S. Shumeiko, and G. Wendin, Phys. Rev. Lett. **74**, 2110 (1995).
[21] D. Averin and A. Bardas, Phys. Rev. Lett. **75**, 1831 (1995).
[22] J. C. Cuevas, A. Martín-Rodero, and A. L. Yeyati, Phys. Rev. B **54**, 7366 (1996).
[23] E. Scheer, N. Agrait, J. C. Cuevas, A. L. Yeyati, B. Ludoph, A. Martin-Rodero, G. Rubio, J. M. van Ruitenbeek, and C. Urbina, Nature (London) **394**, 154 (1998).
[24] R. A. Phillips and A. V. Gold, Phys. Rev. **178**, 932 (1969).
[25] P. M. Everett and C. G. Grenier, Phys. Rev. B **18**, 4477 (1978).
[26] D. A. Gorokhov and P. W. Brouwer, Phys. Rev. Lett. **91**, 186602 (2003).

[27] J. J. Riquelme, L. de la Vega, A. L. Yeyati, N. Agrait, A. Martin-Rodero, and G. Rubio-Bollinger, Europhys. Lett. **70**, 663 (2005).

[28] See Supplemental Material at http://link.aps.org/supplemental/10.1103/PhysRevLett.109.237003 for details of the model used and the calculations, and additional experimental results.

[29] J. G. Rodrigo, V. Crespo, and S. Vieira, Physica (Amsterdam) **437–438C**, 270 (2006).

[30] The MAR spectrum of an helical channel interrupted by a normal wire, as expected at the edge of a 2D topological insulator, has been considered in D. M. Badiane, M. Houzet, and J. S. Meyer, Phys. Rev. Lett. **107**, 177002 (2011). The system considered here analyzes two spin channels coupled by a magnetic field and the spin-orbit interaction, as expected in a metal such as Pb.

[31] H.-J. Kwon, K. Sengupta, and V. M. Yakovenko, Eur. Phys. J. B **37**, 349 (2003).

[32] A. C. Potter and P. A. Lee, Phys. Rev. B **85**, 094516 (2012).

[33] R. F. Service, Science **332**, 193 (2011).

[34] J. Alicea, Rep. Prog. Phys. **75**, 076501 (2012).

[35] V. Mourik, K. Zuo, S. M. Frolov, S. R. Plissard, E. P. A. M. Bakkers, and L. P. Kouwenhoven, Science **336**, 1003 (2012).